Journal of Pharmaceutical and Biomedical Analysis 49 (2009) 18–25

Contents lists available at ScienceDirect

Journal of Pharmaceutical and Biomedical Analysis

journal homepage: www.elsevier.com/locate/jpba

Quantitative solid-state analysis of three solid forms of ranitidine hydrochloride in ternary mixtures using Raman spectroscopy and X-ray powder diffraction

Norman Chieng, Sönke Rehder, Dorothy Saville, Thomas Rades, Jaakko Aaltonen*

School of Pharmacy, University of Otago, Dunedin, New Zealand

ARTICLE INFO

Article history:
Received 20 June 2008
Received in revised form
23 September 2008
Accepted 23 September 2008
Available online 17 October 2008

Keywords:
Solid state
Ranitidine HCl
Polymorphism
Amorphous
Quantification
Multivariate analysis
Principal component analysis (PCA)
Partial least squares (PLS) regression
Raman spectroscopy
X-ray powder diffraction

ABSTRACT

The aim of the study was to develop a reliable quantification procedure for mixtures of three solid forms of ranitidine hydrochloride using X-ray powder diffraction (XRPD) and Raman spectroscopy combined with multivariate analysis. The effect of mixing methods of the calibration samples on the calibration model quality was also investigated. Thirteen ternary samples of form 1, form 2 and the amorphous form of ranitidine hydrochloride were prepared in triplicate to build a calibration model. The ternary samples were prepared by three mixing methods (a) manual mixing (MM) and ball mill mixing (BM) using two (b) 5 mm (BM5) or (c) 12 mm (BM12) balls for 1 min. The samples were analyzed with XRPD and Raman spectroscopy. Principal component analysis (PCA) was used to study the effect of mixing method, while partial least squares (PLS) regression was used to build the quantification models. PCA score plots showed that, in general, BM12 resulted in the narrowest sample clustering indicating better sample homogeneity. In the quantification models, the number of PLS factors was determined using cross-validation and the models were validated using independent test samples with known concentrations. Multiplicative scattering correction (MSC) without scaling gave the best PLS regression model for XPRD, and standard normal variate (SNV) transformation with centering gave the best model for Raman spectroscopy. Using PLS regression, the root mean square error of prediction (RMSEP) values of the best models were 5.0–6.9% for XRPD and 2.5–4.5% for Raman spectroscopy. XRPD and Raman spectroscopy in combination with PLS regression can be used to quantify the amount of single components in ternary mixtures of ranitidine hydrochloride solid forms. Raman spectroscopy gave better PLS regression models than XRPD, allowing a more accurate quantification.

1. Introduction

Pharmaceutical solids are known to exhibit polymorphism. It is also well recognised that different polymorphic forms can have differences in pharmaceutically relevant properties such as stability, solubility and bioavailability [1]. During pharmaceutical development and manufacturing, changes in the solid state can occur including polymorphic transformation, formation or dehydration/desolvation of a hydrate/solvent, conversion from crystalline to amorphous phase or vice versa, and all of these can significantly alter the drug product performance [2]. Thus monitoring solid-state properties, both qualitative and quantitative, is important in order to ensure high quality products [3].

Over the years, a variety of analytical techniques have been successfully used for quantitative solid-state analysis including X-ray powder diffraction (XRPD), differential scanning calorimetry (DSC), Raman [1] and Fourier transform infrared spectroscopy [4], solid-state nuclear magnetic resonance [5] and terahertz pulsed spectroscopy [6]; typically in the context of binary mixtures (crystalline/amorphous or crystalline/crystalline). In this study, XRPD and Raman spectroscopy were employed. XRPD gives fundamental structural information, while Raman spectroscopy provides an insight into the solid materials at the molecular level [7]. Both techniques are non-destructive, easy and relatively fast to use [2]. To date, few studies have been carried out to quantify multiple solid forms (i.e. ≥3) in a mixture using spectroscopic techniques [4,8]. To the best of our knowledge, there are no studies investigating the ability of XRPD to quantify solid forms in ternary mixtures. Conventionally, quantitative analysis of pharmaceutical solids has been done by employing uni- or bivariate approaches based on either the heights or areas of a single or several characteristic peaks [9–11]. Although uni- or bivariate methods are simple to use, they are often not feasible due to complicated spectra with overlapping

* Corresponding author currently at: Department of Pharmaceutics, University of Kuopio, P.O. Box 1627, FIN-70211, Kuopio, Finland. Tel.: +358 40 355 3872; fax: +358 17 162 252.
E-mail address: jaakko.aaltonen@uku.fi (J. Aaltonen).

0731-7085/$ – see front matter © 2008 Elsevier B.V. All rights reserved.
doi:10.1016/j.jpba.2008.09.054

peaks, or as is the case of XRPD patterns of amorphous materials, the absence of peaks. A Raman spectrum of an amorphous material is known to have broadened and overlapping spectral bands when compared to the crystalline counterparts [12]. To overcome these problems, multivariate methods that use the whole spectral information instead of only few peaks can be used. In partial least squares (PLS) regression, the covariance between the variables *X* (i.e. whole diffractogram or spectrum) and *Y* (i.e. concentration) is maximised to extract as much information as possible, while the unrelated data is ignored [13]. This enables PLS regression to simultaneously analyze and quantify mixtures containing several components with no available peaks or with overlapping peaks [14].

Ranitidine hydrochloride was used as a model compound. It is known to exist in two polymorphic forms, form 1 and form 2 and an amorphous form [15]. The physicochemical properties and the stability of the solid forms are well characterized and can be found elsewhere [16,17]. Both form 1 and form 2 are bioequivalent and are available in formulated drug products. Regardless of the fact that both forms are bioequivalent, interest has been given to both forms for intellectual property reasons [18].

The objective of the study was to develop reliable quantification procedures for the mixtures of three solid forms of ranitidine hydrochloride using XRPD and Raman spectroscopy combined with multivariate analysis. In addition, the effect of different mixing methods of the calibration samples was investigated. Multivariate analysis, specifically principal component analysis (PCA) and PLS regression combined with various pre-processing algorithms and scaling methods were used for the analysis of diffractograms/spectra.

2. Materials and methods

2.1. Materials

Ranitidine hydrochloride form 1 (Salutas Pharma, Germany. Batch: 105293/40011298) and ranitidine hydrochloride form 2 (Salutas Pharma, Germany. Batch: 556314/10191475) were used as raw materials.

2.2. Methods

2.2.1. Sample preparation of crystalline ranitidine hydrochloride form 1 and form 2

To prepare solid forms with uniform particle size, the raw materials of form 1 and form 2 were lightly ground in a mortar. The solids were then stored at 70 °C for 24 h to remove adsorbed water. After grinding, XRPD was used to verify no polymorphic transformations occurred during the grinding (see Section 2.3.1 for details).

2.2.2. Sample preparation of amorphous ranitidine hydrochloride

Amorphous ranitidine hydrochloride was prepared by cryo-milling ranitidine hydrochloride form 1 in an oscillatory ball mill (MM 301, Retsch GmbH & Co., Germany) at 25 Hz. 1 g of powder was placed in a 25-ml milling chamber with two 12 mm stainless steel balls. The milling chambers were then sealed and immersed in liquid nitrogen for three min before milling for 60 min. Re-cooling of the milling chambers was carried out every 20 min. XRPD was used to confirm the sample was 100% X-ray amorphous (only a halo and no peaks were present in the XRPD pattern). DSC thermograms also showed glass transition and crystallization events (data not shown) indicating the cryo-milled sample was amorphous. The cryo-milled samples were stored in an airtight container over silica gel at −20 °C until required. The amorphous samples were used within 2 days for the preparation of ternary mixtures.

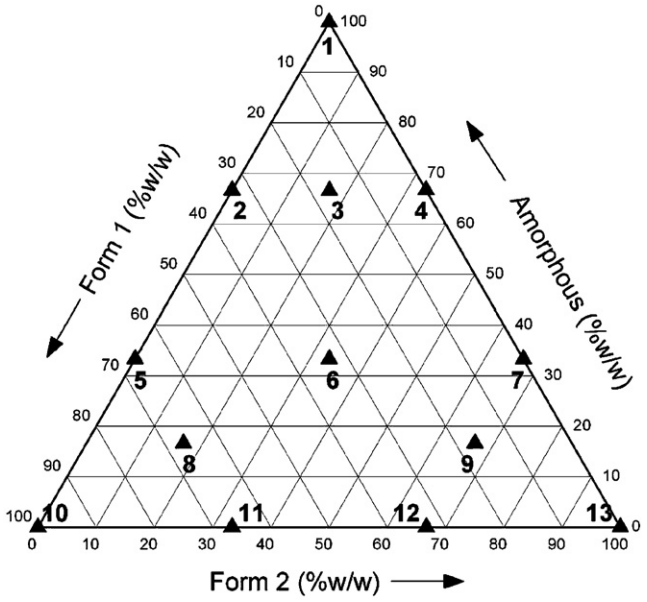

Fig. 1. Ternary diagram showing the 13 mixtures of ranitidine hydrochloride form 1, form 2 and amorphous form used.

2.2.3. Preparation of ternary calibration and test samples

Thirteen ternary mixtures of ranitidine hydrochloride form 1, form 2 and amorphous ranitidine hydrochloride were selected based on the triangle experimental design. The ratios (form 1:form 2:amorphous) were (1:0:0), (0:1:0), (0:0:1), (2/3:1/3:0), (2/3:0:1/3), (0:2/3:1/3), (0:1/3:2/3), (1/3:0:2/3), (1/3:2/3:0), (1/3:1/3:1/3), (2/3:1/6:1/6), (1/6:2/3:1/6) and (1/6:1/6:2/3) as illustrated in Fig. 1.

The calibration samples (m = 600 mg) were prepared in a cold room (4 °C) by manual mixing (MM) and two different ball mill mixing (BM) methods. In the MM method, the solid forms at appropriate ratios were mixed gently for 1 min using a miniature glass mortar and pestle. In the BM method, the solid forms were weighed into a 25-ml milling chamber and either two 5 mm (BM5) or 12 mm (BM12) stainless steel balls were used to mix the samples. The ternary mixtures were mixed for 1 min at 25 Hz. The prepared samples were then stored in an airtight container over silica gel at −20 °C. Measurements by XRPD and Raman spectroscopy were performed on the same sample within 2 days of sample preparation. All ratios were prepared and analyzed in triplicate.

2.3. Characterization

2.3.1. X-ray powder diffraction

XRPD analysis was performed using an X'Pert PRO X-ray diffractometer (PANalytical, The Netherlands; MPD PW3040/60 XRD; CuKα anode; λ = 1.541 Å). The samples were gently consolidated in an aluminium holder and scanned at 40 kV and 30 mA from 5 to 35° 2θ using a scanning speed of 0.1285° min^{-1} and a step size of 0.0084°. The diffraction patterns were analyzed using X'Pert High Score software (version 2.2.0) and plotted using OriginPro 7.0 (OriginLab Corporation, USA).

2.3.2. Raman spectroscopy

The FT-Raman instrument consisted of a Bruker FRA 106/S FT-Raman accessory (Bruker Optik, Ettlingen, Germany) with a Coherent Compass 1064-500N laser (Coherent Inc., Santa Clara, USA) attached to a Bruker IFS 55 FT-IR interferometer, and a D 425 Ge diode detector. Analysis was carried out at room temperature

utilizing a laser wavelength of 1064 nm (Nd:YAG laser) and a laser power of 120 mW. Back-scattered radiation was collected at an angle of 180°. Samples were measured in aluminium cups and 32 scans were averaged for each sample at a resolution of 4 cm^{-1}. Sulphur was used as a reference standard to monitor the wavenumber accuracy. OPUS^{TM} 5.0 (Bruker Optik, Ettlingen, Germany) was used for the spectral analysis.

2.3.3. Standard and modulated differential scanning calorimetry (DSC and MDSC)

DSC was used to probe the presence of amorphous drug in the ternary samples after mixing. The measurements (sample powders of 1–3 mg crimped in a standard aluminum pan) were carried out using a DSC Q100 (v8.2 Build 268, TA Instruments, USA) at a heating rate of 10 K per min from 0 to 160 °C under a nitrogen gas flow of 50 ml/min. In MDSC, the samples were heated at a heating rate of 5 K per min from −10 to 40 °C. The modulation amplitude was 0.5 °C and the period was 60 s. Calibration of the DSC instrument was performed using indium as a standard.

2.4. Multivariate data analysis

The suitability of various mixing methods was evaluated by PCA. PCA score plots were used to compare clustering of the XRPD diffractograms and Raman spectra of the ternary samples. The XRPD score plots were obtained after the diffractograms were centered. Pre-processing algorithms were not applied here to avoid losing relevant information [19]. In Raman spectroscopic PCA score plots, the variables were standard normal variate (SNV) transformed and centred prior to clustering analysis. SNV transformation combined with centering has been shown to improve the Raman spectral analysis [20,21].

PLS regression was used to create calibration models for quantitative analysis. For each XRPD calibration model (MM, BM5 and BM12) 39 diffractograms (13 ternary mixtures in triplicate) were used. In Raman spectroscopic calibration models 117 spectra (13 ternary mixtures in triplicate, each sample × 3 spectra) were used to build each model. Both the diffractograms and spectra were subjected to two pre-processing methods, multiplicative scattering correction (MSC) and SNV transformation. The PLS regression model of raw data (i.e. without pre-processing) was also created to compare with pre-processed data. Both MSC and SNV transformation were used to correct the baseline shifting and tilting due to noise and background effects. The difference between MSC and SNV transformation is that MSC requires a 'reference' spectrum (typically the mean spectrum of the calibration data), whereas in SNV transformation, each spectrum is normalized by the standard deviation of the responses across the entire spectral range [22]. To further improve the model quality, three scaling methods were applied in combination with the pre-processed data, namely no scaling (none), centering (CTR), and scaling to unit variance (UV). In CTR, the variables were mean centered but not scaled. In UV, all X-variables were mean centered and scaled to its standard deviation, which gives all the variables equal importance. The number

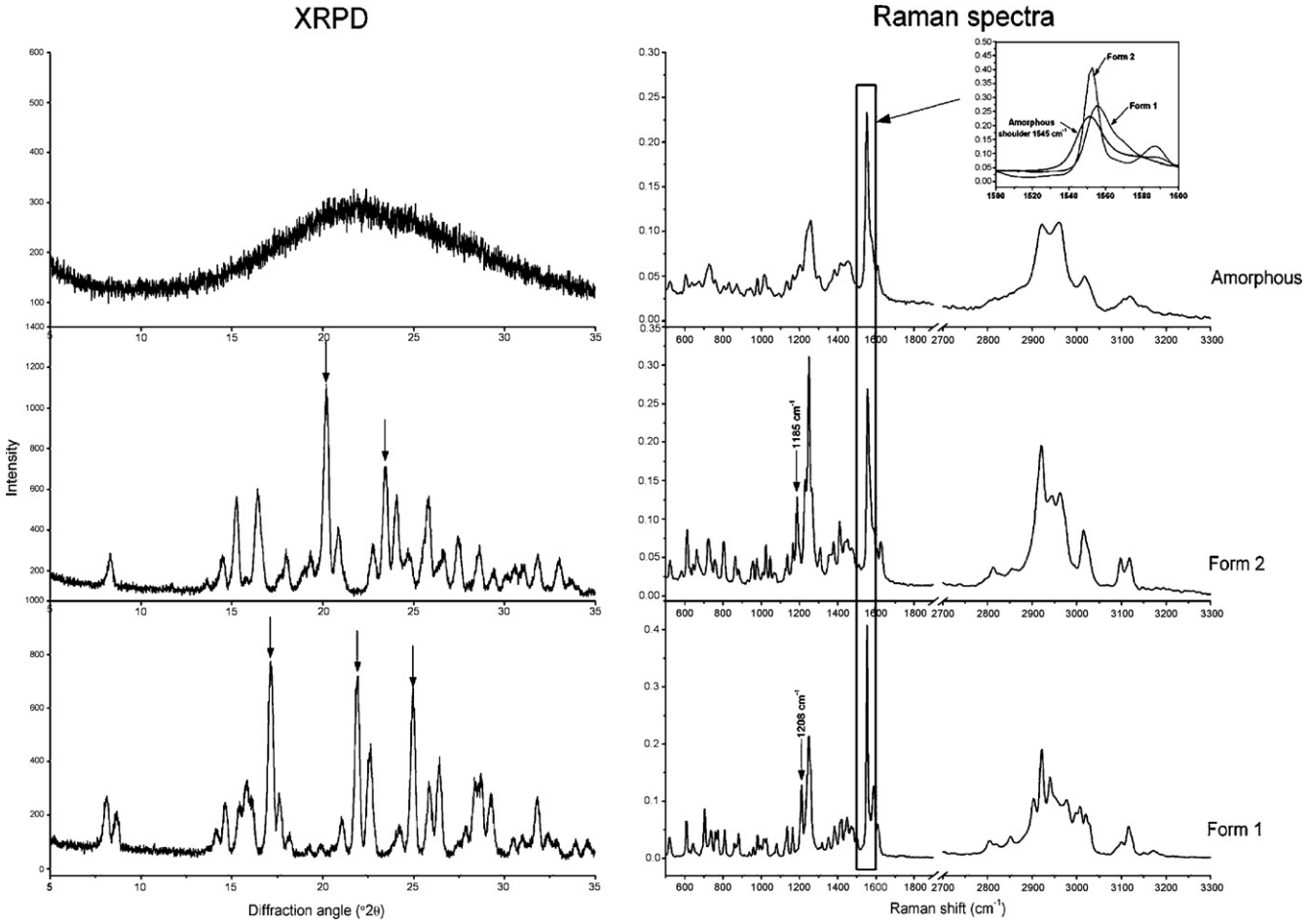

Fig. 2. XRPD diffractograms and Raman spectra of form 1, form 2 and amorphous ranitidine hydrochloride. The arrows indicate the characteristic peaks of form 1 and form 2. Figure inset shows the Raman spectral region between 1500–1600 cm^{-1}, highlighting the differences between form 1, form 2 and amorphous ranitidine hydrochloride.

of PLS factors for each model was determined by cross-validation. Nine independent samples containing solid forms of ranitidine hydrochloride at different concentration ratios, prepared using the procedures from each mixing method were used to test the calibration model. The quality of the model was evaluated by using the correlation coefficient (R^2), test set validation coefficient (Q^2), root mean square error of estimation (RMSEE) and root mean square error of prediction (RMSEP). The data analysis was performed by SIMCA-P (version 11, Umetrics AB, Sweden).

3. Results

3.1. Characterization of crystalline and amorphous state of ranitidine hydrochloride

Fig. 2 shows the XRPD diffractograms and Raman spectra of form 1, form 2 and amorphous ranitidine hydrochloride. Peaks at 17.0, 21.8 and 24.9° 2θ are specific for form 1, while 20.2 and 23.5° 2θ are peaks of form 2. Amorphous ranitidine hydrochloride showed a typical halo diffractogram. In the Raman spectra, the peaks at 1208 and 1185 cm^{-1} can be used to identify form 1 and form 2, respectively. Clear spectral differences of the two crystalline drugs can also be observed in other regions. The spectral peaks of amorphous ranitidine hydrochloride show some similarity to those of the crystalline forms. However, because of the molecular disorder in the amorphous state, the peaks are broader and have extensive overlapping regions. Only a shoulder (at 1545 cm^{-1}) of a peak at 1550 cm^{-1} that corresponds to amorphous ranitidine hydrochloride does not overlap with the crystalline peaks (Fig. 2 inset). Furthermore, neither the 1208 cm^{-1} nor 1185 cm^{-1} peak is present. Whole XRPD patterns (6–34° 2θ) and Raman spectral regions (1000–1700 cm^{-1} and 2700–3250 cm^{-1}) were used to create clustering (PCA) and quantification (PLS regression) models.

3.2. Comparison of mixing techniques

Fig. 3(a and b) shows the PCA score plots of the 13 ternary mixtures prepared by MM, BM5 and BM12, analyzed by XRPD and Raman spectroscopy, respectively. Overall, the triangular shape of the experimental design (Fig. 1) could be observed in the score plots (Fig. 3(a and b), triangle design in dotted line). Comparing the three mixing methods within each analytical technique, it was apparent that MM (Fig. 3(a and b), black triangle) had the most spread clusters, followed by BM5 (green triangle) and BM12 (red triangle). The improvement of the clustering was visible in the XRPD score plots, but was more obvious in the score plots obtained from the Raman spectral PCA, where the BM12 yielded the narrowest clusters. A narrow cluster indicates a homogeneous sample, while a spread cluster suggests a heterogeneous mix. Interestingly, the size of the triangle design diagram (i.e. Fig. 1) for the XRPD BM5 and BM12 score plots were slightly smaller. A trend was observed that the points were moving towards the amorphous form. The shift was most profound for samples containing high amount of crystalline forms (samples 10–13) and were mixed by the BM12 method (Fig. 3(a); red dotted line). A closer observation of the individual diffractograms clearly showed a decrease in the peak intensity of the BM samples compared with the MM samples (Fig. 4; sample point 11), explaining the shifts. In contrast, this shift was not evident on the score plots obtained by Raman spectroscopy (Fig. 3(b)). In addition, neither a glass transition nor a crystallization temperature was observed on the DSC thermograms of the fully crystalline BM5 and BM12 samples (Fig. 5; sample point 11), indicating no amorphous phase was formed. However, an earlier onset of the melting endotherm could be observed, possibly as a result of smaller particle size. Further explanation of this finding is given in Section 4.

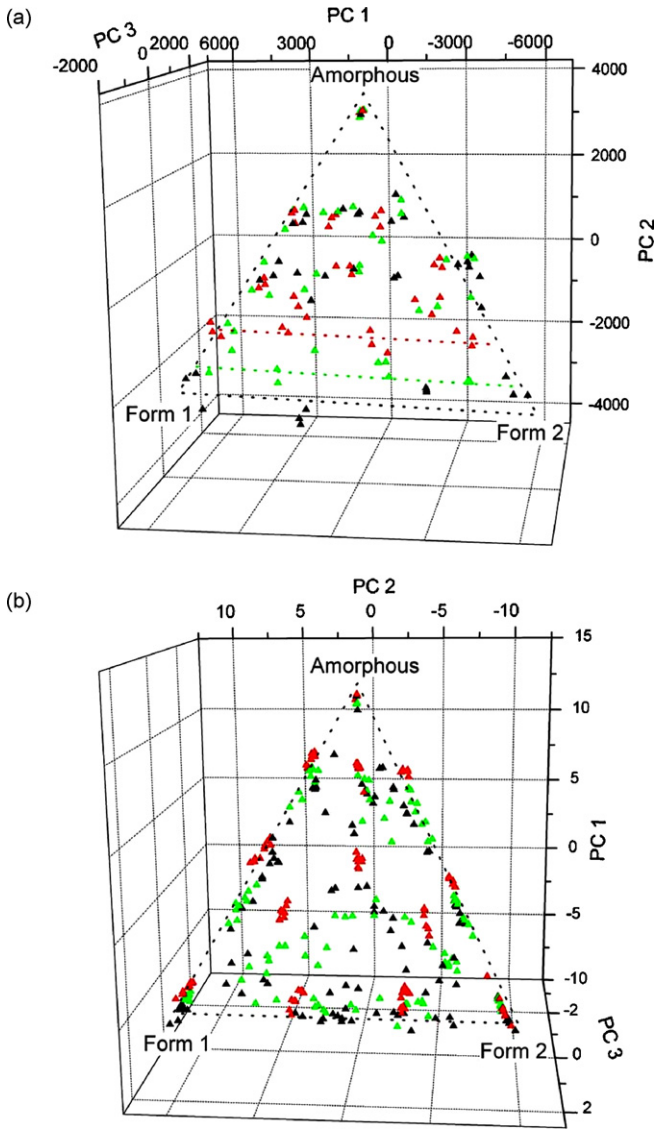

Fig. 3. PCA score plots of (a) XRPD diffractograms and (b) Raman spectra. Each coloured symbol represents a diffractogram or a spectrum. The black, green and red symbols indicate the three mixing methods by MM, BM5 and BM12, respectively. The shift from crystalline towards amorphous samples noticed with XRPD when using BM is indicated by the coloured dotted lines. (For interpretation of the references to colour in this figure legend, the reader is referred to the web version of the article.)

In general, PCA was able to differentiate the two polymorphic forms (crystalline) and the amorphous form based on the first two principal components (PCs). Looking at XRPD PCA loadings (Fig. 6(a)), PC 1 differentiated between form 1 (downward peaks) and form 2 (upward peaks), while PC 2 accounted for the differences between the amorphous form (halo shaped loadings) and crystalline forms (upwards peaks). Similarly, but in a different order, PC 1 in Raman loadings (Fig. 6(b)) differentiated the two crystalline (upward peaks at 1185 and 1208 cm^{-1}) and amorphous form (downward peak at 1545 cm^{-1}) while PC 2 accounted for the differences between form 1 (upward peak at 1208 cm^{-1}) and form 2 (downward peak at 1185 cm^{-1}). The third PC for both XRPD and Raman spectroscopy appeared to account mainly for the peak intensity differences within the diffractograms/spectra. The loadings of both PC 3's were relatively low and had a residual-peak pattern similar to PC 1 or 2 (Fig. 6(a and b)).

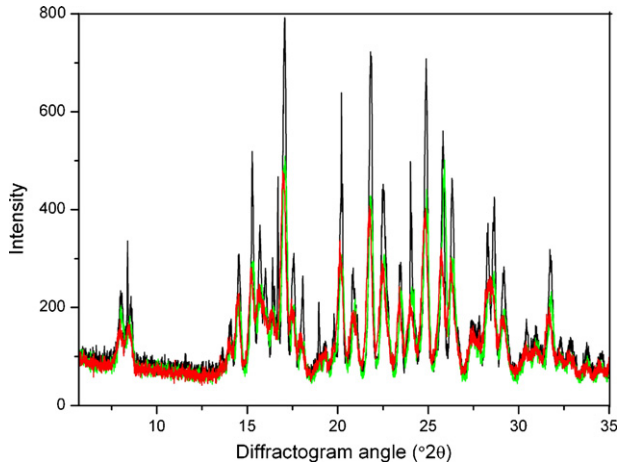

Fig. 4. Comparison of XRPD peak intensity (sample point 11 from the ternary diagram in Fig. 1) of MM (black line), BM5 (green line) and BM12 (red line). (For interpretation of the references to colour in this figure legend, the reader is referred to the web version of the article.)

3.3. Quantification by XRPD

Table 1 presents the results of the PLS regression models of MM, BM5 and BM12 samples constructed using XRPD data. Overall the quality and the performance of the models according to R^2 and Q^2 were relatively good with all the values greater than 0.922 and 0.902, respectively. In the MM samples, cross validation determined that up to 5 PLS factors were required to construct a reliable model. When the ternary mixtures were mixed by BM methods, on average, the number of PLS factors required was reduced to 3 or 4. According to Table 1, the best calibration model was achieved when the BM12 calibration samples were subjected to MSC transformation, without scaling. The RMSEE values ranged from 4.6 to 6.5% and RMSEP values between 5.0 and 6.9%.

Although the BM12 samples combined with MSC transformation and no scaling yielded the best model, no specific correlation could be found between the mixing technique and the pre-processing and scaling methods to obtain a superior quantitative

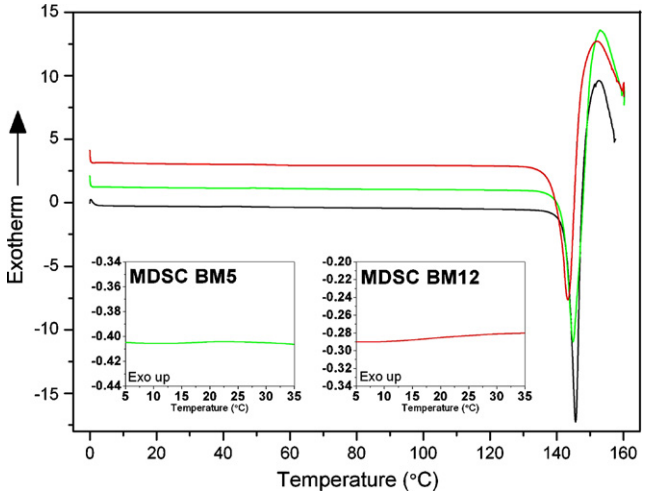

Fig. 5. DSC thermograms of sample point 11 in the ternary diagram (Fig. 1) prepared using different mixing methods MM (black line), BM5 (green line) and BM12 (red line). The thermograms are offset for clarity. Figure insets show the reversing heat flow thermograms obtained with MDSC of sample point 11 prepared by BM5 and BM12. (For interpretation of the references to colour in this figure legend, the reader is referred to the web version of the article.)

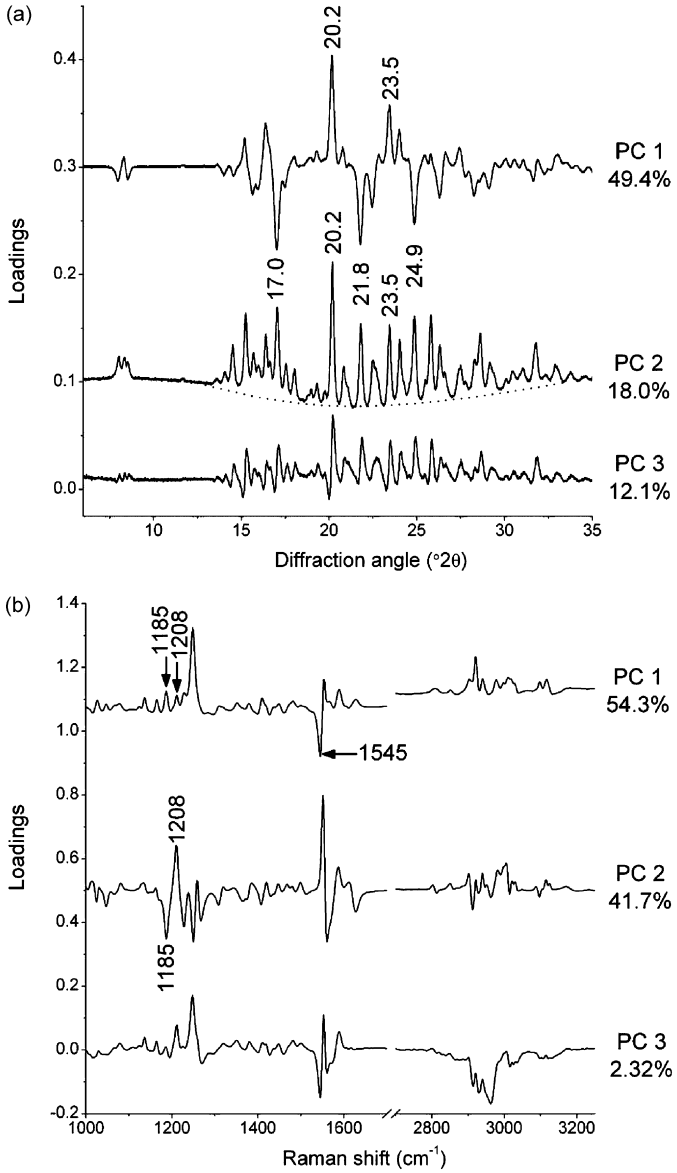

Fig. 6. PCA loading plots of (a) XRPD diffractograms and (b) Raman spectra. The numbers and arrows in the loading plots indicate the characteristics of ranitidine hydrochloride polymorphs. The dotted line in XRPD loadings indicates the halo pattern of the amorphous form. The loading plots are offset for clarity.

model. On the other hand, RMSEE and RMSEP seemed to have a narrower estimation and prediction window when the samples were better mixed using the BM12 method.

3.4. Quantification by Raman spectroscopy

Table 2 presents the results of the PLS regression models constructed using the selected regions of the Raman spectra. Exclusion of the baseline region between 2000 and 2700 cm^{-1} and regions below 1000 cm^{-1} and above 3250 cm^{-1} resulted in a slight improvement of the models compared to using whole spectra. Overall all PLS regression models had R^2 and Q^2 values greater than 0.921 and 0.911, respectively. In the MM samples, 4 PLS factors were required for the non-pre-processed, non-scaled spectra yet the RMSEP values were still extremely high (up to 33%). Applying MSC or SNV transformation to the MM samples followed by scaling by UV or CTR reduced the number of PLS

Table 1
Performance of the XRPD PLS regression models using different mixing, pre-processing and scaling methods.

Mixing methods	Pre-processing methods	Scaling	# PLS Factors	R^2	Q^2	Amorphous		Form 1		Form 2	
						RMSEE (%)	RMSEP (%)	RMSEE (%)	RMSEP (%)	RMSEE (%)	RMSEP (%)
MM	None	None	4	0.985	0.979	4.8	7.4	5.3	7.3	7.3	6.5
		UV	3	0.975	0.968	4.9	9.2	3.6	4.6	6.6	6.6
		CTR	3	0.971	0.955	5.6	8.0	4.6	5.8	6.4	7.0
	SNV	None	3	0.955	0.947	6.3	12.8	11.3	12.4	11.8	17.0
		UV	5	0.974	0.935	4.8	11.9	5.6	16.7	5.9	18.1
		CTR	3	0.944	0.902	5.4	12.5	6.8	9.0	10.3	13.8
	MSC	None	3	0.963	0.955	10.0	13.8	8.0	7.0	9.5	12.2
		UV	5	0.982	0.934	3.8	17.2	3.7	7.2	5.8	13.2
		CTR	2	0.922	0.906	9.9	13.8	7.9	7.0	9.3	12.2
BM5	None	None	3	0.973	0.969	4.8	11.5	6.8	6.2	10.5	8.6
		UV	3	0.981	0.974	4.0	8.2	4.2	2.6	5.4	7.3
		CTR	3	0.970	0.961	5.6	11.6	4.3	5.6	6.9	8.5
	SNV	None	3	0.961	0.955	8.8	9.2	9.9	9.5	9.8	11.2
		UV	3	0.947	0.918	7.1	9.2	8.4	8.8	7.3	10.1
		CTR	4	0.961	0.942	6.0	11.4	7.1	8.1	6.7	9.0
	MSC	None	3	0.969	0.965	10.4	10.4	7.6	6.1	7.0	8.0
		UV	4	0.974	0.948	4.5	13.2	5.4	7.7	6.3	10.3
		CTR	2	0.934	0.927	10.3	10.4	7.5	6.1	6.9	8.0
BM12	None	None	4	0.983	0.972	6.8	5.2	5.9	8.1	6.4	12.4
		UV	4	0.984	0.967	4.7	4.7	3.4	4.9	4.2	2.9
		CTR	2	0.957	0.954	8.5	9.7	4.4	9.4	6.8	5.3
	SNV	None	4	0.977	0.970	5.5	5.2	8.6	9.7	7.8	8.0
		UV	3	0.974	0.956	5.3	6.0	5.5	7.5	5.3	8.1
		CTR	3	0.969	0.956	5.5	5.3	5.9	6.8	6.2	6.5
	MSC	None	4	0.987	0.983	6.5	6.9	4.6	5.4	5.2	5.0
		UV	3	0.984	0.971	4.7	9.0	3.7	7.6	4.3	6.7
		CTR	3	0.973	0.964	6.5	6.9	4.5	5.4	5.1	5.0

MM: manual mixing; BM5: ball mill mixing using two 5 mm stainless steel balls; BM12: ball mill mixing using two 12 mm stainless steel balls; SNV: standard normal variate transformation; MSC: multiplicative scattering correction; UV: unit variance scaling; CTR: centering; RMSEE: root mean square error of estimation; RMSEP: root mean square error of prediction.

Table 2
Performance of the Raman spectroscopic PLS regression models using different mixing, pre-processing and scaling methods.

Mixing methods	Pre-processing methods	Scaling	# PLS Factors	R^2	Q^2	Amorphous		Form 1		Form 2	
						RMSEE (%)	RMSEP (%)	RMSEE (%)	RMSEP (%)	RMSEE (%)	RMSEP (%)
MM	None	None	4	0.952	0.951	9.0	29.6	12.3	15.7	8.9	16.1
		UV	4	0.921	0.912	8.2	32.9	10.9	20.1	9.0	18.9
		CTR	4	0.927	0.918	7.7	26.9	9.6	16.4	8.4	17.4
	SNV	None	4	0.969	0.968	7.9	6.5	8.8	6.0	8.3	7.4
		UV	3	0.935	0.933	7.1	7.0	9.1	9.0	7.9	7.8
		CTR	3	0.935	0.932	7.0	6.8	9.0	8.8	8.2	8.1
	MSC	None	4	0.971	0.969	6.8	10.8	8.9	8.2	8.1	10.5
		UV	3	0.937	0.935	6.7	16.0	9.0	8.6	8.0	14.0
		CTR	3	0.937	0.934	6.7	11.1	8.9	8.2	8.1	10.4
BM5	None	None	3	0.952	0.950	8.9	6.0	12.7	11.2	8.3	13.0
		UV	4	0.942	0.911	6.1	7.4	9.2	9.0	7.4	10.4
		CTR	4	0.943	0.930	6.2	7.8	9.1	8.6	7.2	10.4
	SNV	None	3	0.977	0.975	6.4	6.4	7.9	6.6	6.8	6.9
		UV	3	0.960	0.959	4.9	6.4	7.5	5.9	6.2	7.1
		CTR	3	0.962	0.958	4.6	6.0	7.4	5.7	6.4	7.1
	MSC	None	3	0.978	0.976	6.4	6.3	7.9	6.7	6.4	6.3
		UV	3	0.961	0.959	5.0	6.8	7.3	5.6	6.4	7.4
		CTR	3	0.962	0.959	4.7	6.1	7.2	5.5	6.3	6.6
BM12	None	None	3	0.967	0.966	8.5	6.1	8.4	9.6	8.3	9.3
		UV	4	0.960	0.949	6.8	7.3	6.6	9.1	5.6	5.7
		CTR	3	0.950	0.945	8.1	6.6	7.2	8.1	5.7	5.5
	SNV	None	3	0.987	0.986	7.2	7.1	5.3	5.6	2.4	2.3
		UV	3	0.986	0.985	4.6	5.6	3.9	3.7	2.5	3.5
		CTR	3	0.987	0.986	4.4	4.5	3.8	3.6	2.3	2.5
	MSC	None	3	0.987	0.986	6.7	6.7	5.9	6.4	5.9	2.5
		UV	3	0.979	0.978	5.6	5.5	4.9	4.6	2.8	3.4
		CTR	3	0.980	0.979	5.4	4.7	4.9	4.5	2.6	2.6

MM: manual mixing; BM5: ball mill mixing using two 5 mm stainless steel balls; BM12: ball mill mixing using two 12 mm stainless steel balls; SNV: standard normal variate transformation; MSC: multiplicative scattering correction; UV: unit variance scaling; CTR: centering; RMSEE: root mean square error of estimation; RMSEP: root mean square error of prediction.

factors required to three, but at the expense of a poorer model according to the R^2 (~0.93). The RMSEP values were halved but were still considerably high (16%). When the samples were mixed by BM methods, the models created were much better (higher R^2 and Q^2) and had a smaller RMSEE and RMSEP compared to the MM models. Further improvement of the ternary calibration model was obtained when the BM mixed samples were subjected to MSC or SNV transformation. Comparing the PLS regression models created by the two BM methods, a better model was obtained when the samples were mixed using 12 mm balls (BM12).

According to Table 2, the best calibration model was achieved when the BM12 samples were subjected to SNV transformation and scaled by CTR (R^2 = 0.987 and Q^2 = 0.986). Two other models, created by MSC and SNV transformation of the BM12 samples, without scaling resulted in similar R^2 and Q^2 values. However, SNV transformation combined with CTR scaling appeared to be superior, as demonstrated by the smaller and narrower range of RMSEE and RMSEP values (RMSEE of 2.3–4.4% and RMSEP of 2.5–4.5%).

4. Discussion

When the three solid forms were mixed by various mixing methods, PCA score plots showed that mixing by BM, in general, produced a narrower cluster, indicating better sample homogeneity. BM12 was superior to BM5. In contrast, samples mixed by MM were spread widely. This finding was not unexpected because previous studies have shown that high energy BM mixing can result in improved powder homogeneity through the formation of fine powder mixtures [23,24]. However, high energy mixing could cause changes in the physical state of the sample [25], and in some cases polymorphic transformation [26]. In this study, XRPD was able to detect a reduction in the peak intensity of BM5 and BM12 samples and thus a shift of scores in the PCA score plot as observed in Fig. 3(a) (green and red dotted lines). However, neither a glass transition nor crystallization was detected on the DSC thermograms (Fig. 5), which confirmed that there was no conversion to amorphous form after 1 min of BM. The absence of a glass transition was further confirmed by MDSC analysis (Fig. 5). Raman spectroscopic PCA score plots (Fig. 3(b)) showed that, regardless of the mixing methods used, no shifting of the scores towards the amorphous form was noticed. In addition the reduction in peak intensity or broadening of peaks was not detected in the Raman spectra upon BM, further confirming the absence of amorphization.

On the other hand, the 'bigger' MM triangle design relative to the BM models in Fig. 3(a) could also be explained by the larger particle size in MM samples, possibly resulting in preferred orientation of the solid powder during sample preparation, leading to higher XRPD peak intensity. Preferred orientation is a well-known limitation of XRPD analysis and can be minimized by grinding the samples [7]. However, reduction in particle size can also cause a broadening of X-ray lines, which in turn affects the peak intensity [7]. According to Raman spectroscopy and DSC analysis, BM5 and BM12 mixing did not result in a change of the crystalline forms towards the amorphous form. Therefore, it is possible that the shift of the crystalline points towards the amorphous points in XRPD ternary diagrams is likely due to particle size diminishing during BM, leading to broadening of the XPRD peaks. Further study is required to evaluate the particle size of the mixtures prepared by the various mixing methods.

Nevertheless, regardless of the mixing method used, both analytical methods combined with PLS regression were found to be almost equally effective in quantifying the solid forms in the ternary mixtures. Applying MSC resulted in a better calibration model with XRPD, whereas SNV transformation combined with centering was the preferred way for the Raman spectroscopic model to lower and narrow the RMSEE and RMSEP values. The best R^2-value for both techniques was 0.987. However, the model quality for Raman spectroscopy stood out slightly, with a Q^2-value of 0.986 compared to 0.983 with XRPD. The RMSEE and RMSEP values of the best XRPD model were between 4.6–6.5% and 5.0–6.9% respectively, while the best Raman spectroscopy model had values between 2.3–4.4% (RMSEE) and 2.5–4.5% (RMSEP). The performance of the XRPD model could not be compared with literature data as, to the best of our knowledge, similar studies have not been published. On the other hand, in a study of ternary solid-state mixtures of indomethacin (two crystalline and the amorphous form) using Raman spectroscopy, the authors reported RMSEP value range of 5.3–6.5% [12]. The best RMSEP range in the current study is slightly better than the previously reported RMSEP range, most likely due to the optimized mixing method (BM12).

Raman spectroscopy appeared to have lower RMSEE and RMSEP values but sample homogeneity was more crucial. Campbell Roberts et al. [1], Heinz et al. [12], and Wang et al. [27] have reported sample homogeneity is one of the major sources of error in the quantification by Raman spectroscopy. In this study, sample homogeneity could be improved by the BM12 method although this process is a little more tedious than MM. Other possible ways to increase sampling homogeneity would be using a rotating sample holder during measurement [28] or a wider area of illumination [29] to increase the effective sampling area. On the other hand, sample homogeneity was not a major issue for XRPD analysis possibly because of the larger sample size (>100 mg). The sample is thus more representative of the mixture and less prone to sub-sampling.

XRPD provides information about the crystal packing and is known as the 'gold standard' technique used in the study of polymorphism. However, although providing mostly intramolecular information, Raman spectroscopy may have advantages over XRPD due to its better accuracy and precision, ability to perform on-line monitoring, higher throughput and a lower cost.

5. Conclusions

BM12 for was found to be the preferred mixing method over MM and BM5. BM12 was sufficient to reduce preferred orientation in XRPD (with some reduction in peak intensity) and to attain good homogeneity in the calibration samples without changing the physical state of the crystalline samples. XRPD and Raman spectroscopy in combination with PLS regression can be used to quantify the amount of solid form components in ternary ranitidine hydrochloride mixtures. XRPD was more sensitive to packing of the powder during sample preparation (preferred orientation), while sample homogeneity was crucial in Raman spectroscopic analysis. Raman spectroscopy gave slightly better PLS regression models than XRPD, allowing a more accurate quantification of the three solid forms of ranitidine hydrochloride.

Acknowledgements

Damian Walls (Dept. of Geology, University of Otago) for helping with XRPD, and Cushla McGoverin and Associate Prof. Keith Gordon (Dept. of Chemistry, University of Otago) for helping with Raman spectroscopy. Thanks to the New Zealand Pharmacy Education Research Foundation (NZPERF) for providing funding, the School of Pharmacy, University of Otago, for providing a stipend for NC and the Academy of Finland, Finnish Cultural Foundation and Finnish Pharmaceutical Society for financial support for JA.

References

[1] S.N. Campbell Roberts, A.C. Williams, I.M. Grimsey, S.W. Booth, J. Pharmaceut. Biomed. Anal. 28 (2002) 1135–1147.

[2] G.A. Stephenson, R.A. Forbes, S.M. Reutzel-Edens, Adv. Drug Del. Rev. 48 (2001) 67–90.
[3] G. Buckton, D. P., Int. J. Pharm., 179 (1999) 141–158.
[4] K. Kipouros, K. Kachrimanis, I. Nikolakakis, V. Tserki, S. Malamataris, J. Pharm. Sci. 95 (2006) 2419–2431.
[5] S. Sanchez, F. Ziarelli, S. Viel, C. Delaurent, S. Caldarelli, J. Pharmaceut. Biomed. Anal. 47 (2008) 683–687.
[6] C.J. Strachan, P.F. Taday, D.A. Newnham, K.C. Gordon, J.A. Zeitler, M. Pepper, T. Rades, J. Pharm. Sci. 94 (2005) 837–846.
[7] H.G. Brittain, Physical Characterization of Pharmaceutical Solids, Marcel Dekker Inc., New York, 1995.
[8] K. Kogermann, J. Aaltonen, C.J. Strachan, K. Pöllänen, J. Heinämäki, J. Yliruusi, J. Rantanen, J. Pharm. Sci. 97 (2008) 4983–4999.
[9] D.E. Bugay, A.W. Newman, W.P. Findlay, J. Pharmaceut. Biomed. Anal. 15 (1996) 49–61.
[10] R. Suryanarayanan, Pharm. Res. 6 (1989) 1017–1024.
[11] R.S. Chao, K.C. Vail, Pharm. Res. 4 (1987) 429–432.
[12] A. Heinz, M. Savolainen, T. Rades, C.J. Strachan, Eur. J. Pharmaceut. Sci. 32 (2007) 182–192.
[13] R. Brereton, Applied Chemometrics for Scientists, John Wiley & Sons Ltd., England, 2007.
[14] J. Gabrielsson, N.-O. Lindberg, T. Lundstedt, J. Chemometr. 16 (2002) 141–160.
[15] N. Chieng, T. Rades, D. Saville, Eur. J. Pharm. Biopharm. 68 (2008) 771–780.
[16] T. Madan, A.P. Kakkar, Drug Dev. Ind. Pharm. 20 (1994) 1571–1588.
[17] M. Mirmehrabi, S. Rohani, K.S.K. Murthy, B. Radatus, J. Cryst. Growth 260 (2004) 517–526.
[18] J. Bernstein, Polymorphism in Molecular Crystals, Oxford University Press, UK, 2002.
[19] K. Pöllänen, A. Häkkinen, S.-P. Reinikainen, J. Rantanen, M. Karjalainen, M. Louhi-Kultanen, L. Nyström, J. Pharmaceut. Biomed. Anal. 38 (2005) 275–284.
[20] J. Aaltonen, C.J. Strachan, K. Pöllänen, J. Yliruusi, J. Rantanen, J. Pharmaceut. Biomed. Anal. 44 (2007) 477–483.
[21] M. Savolainen, A. Heinz, C. Strachan, K.C. Gordon, J. Yliruusi, T. Rades, N. Sandler, Eur. J. Pharmaceut. Sci. 30 (2007) 113–123.
[22] M. Zeaiter, J.M. Roger, V. Bellon-Maurel, Trends Anal. Chem. 24 (2005) 437–445.
[23] I. Krycer, J.A. Hersey, Powder Technol. 27 (1980) 137–141.
[24] E. Sallam, N. Orr, Drug Dev. Ind. Pharm. 11 (1985) 607–633.
[25] H. Li, J.G. Stowell, X. He, K.R. Morris, S.R. Byrn, J. Pharm. Sci. 96 (2007) 1079–1089.
[26] N. Chieng, Z. Zujovic, G. Bowmaker, T. Rades, D. Saville, Int. J. Pharm. 327 (2006) 35–44.
[27] H.L. Wang, C.K. Mann, T.J. Vickers, Appl. Spectrosc. 56 (2002) 1538–1544.
[28] F.W. Langkilde, J. Sjoblom, L. Tekenbergs-Hjelte, J. Mrak, J. Pharmaceut. Biomed. Anal. 15 (1997) 687–696.
[29] M. Kim, H. Chung, Y. Woo, M. Kemper, Anal. Chim. Acta 579 (2006) 209–216.